General Disclaimer

One or more of the Following Statements may affect this Document

- This document has been reproduced from the best copy furnished by the organizational source. It is being released in the interest of making available as much information as possible.

- This document may contain data, which exceeds the sheet parameters. It was furnished in this condition by the organizational source and is the best copy available.

- This document may contain tone-on-tone or color graphs, charts and/or pictures, which have been reproduced in black and white.

- This document is paginated as submitted by the original source.

- Portions of this document are not fully legible due to the historical nature of some of the material. However, it is the best reproduction available from the original submission.

Produced by the NASA Center for Aerospace Information (CASI)
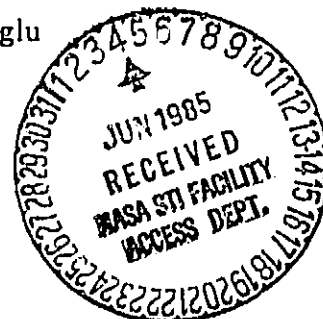
Semiannual Progress Report

for

SIMULATION STUDIES FOR SURFACES AND MATERIALS STRENGTH

November 1, 1984 - April 30, 1985

Cooperative agreement No: NCC 2-297

Period of award: May 1, 1984 - April 30, 1987

Principal investigator: Timur Halicioglu

Eloret Institute
1178 Maraschino Drive
Sunnyvale, CA 94087

Investigations were carried out to analyze various properties of materials employing computer simulation techniques based on semiempirical potential functions which comprises two-body and three-body interactions. In the following three 'self contained' chapters we outlined the basic procedures employed and the advances made during this period .

The first chapter involves an analysis of the relationship between the thermodynamic stability and the parameters of the semiempirical potential energy function employed in the simulation calculations. It contains a detailed investigation of the structural transformations from Diamond Cubic $\Rightarrow$ β-tin and from Graphite $\Rightarrow$ Diamond Cubic which occur at high pressures. Also, in this chapter the surface reconstruction of the (100), (110) and (111) planes for the diamond cubic crystal was analyzed and a marked contraction of the first surface layer spacings was found. Furthermore, it was found that the reduced surface tension, σ^*, decreases with increase of Z^*, the three-body intensity parameter, for all three planes and falls in the expected experimental range.

The second chapter involves a parametric analysis of the elastic constants and the mechanical stability of cubic structures against all types of homogeneous elastic deformations. The domain of absolute stability, involving simultaneous thermodynamic and mechanical stability for fcc, bcc, diamond cubic and simple cubic structures were determined using a potential energy function based on two- and three-body interactions.

In the last chapter, specific parameters involved in two-body plus three-body semiempirical potential energy function for carbon, silicon and silicon carbide systems were calculated. Excellent reproduction for various energetics and structural quantities were obtained.

These three chapters were prepared as separate manuscripts and submitted for publication.

Chapter I

A STUDY OF CRYSTAL STABILITY AND SURFACE ENERGY
FOR DIAMOND CUBIC STRUCTUTRES

INTRODUCTION

From intermolecular force studies, it is now known that the overall non-additive contribution to the lattice energy is positive so that analysis based on only pairwise additivity suggests a shallower intermolecular potential than the true value[1]. Two body contributions alone are also know to be categorically unable to even qualitatively describe some configurations of molecular clusters in the gas phase[2] or the general relaxation and reconstruction of fcc crystal surfaces[3]. In addition, the many-body contribution has been shown to play a key role in the stability of certain crystal structures[4].

In these recent analyses[2-4], a relatively simple potential energy function (PEF), comprising only a two-body Mie-type potential plus a three-body Axilrod-Teller-type potential, was found to be extremely effective. In the present paper, this same parametric PEF is applied to describe the bulk stability and surface energy for the diamond cubic structure. To test the stability condition, the FCC, BCC, diamond cubic, graphite and β-tin structures were considered. For the surface energy study, only the (111), (100) and (110) planes of the diamond cubic structure were considered.

ANALYTICAL PROCEDURE

The PEF, ϕ, is given as[4]

$$\Phi = \psi_2 + \psi_3 \qquad (1a)$$

where

$$\psi_2 = \frac{1}{2} \sum_{\substack{i \\ i \neq j}}^{N} \sum_{j}^{N} \frac{\epsilon}{m-n} \left[n\left(\frac{r_0}{r_{ij}}\right)^m - m\left(\frac{r_0}{r_{ij}}\right)^n \right] \qquad (1b)$$

and

$$\psi_3 = \frac{1}{6} \sum_{\substack{i \\ i \neq j \neq k}}^{N} \sum_{j}^{N} \sum_{k}^{N} Z \frac{(1 + 3 \cos \theta_i \cos \theta_j \cos \theta_k)}{(r_{ij} \, r_{ik} \, r_{jk})^3} . \qquad (1c)$$

In eq. (1b), $r_{ij} = |\vec{r}_i - \vec{r}_j|$, r_0 denotes the equilibrium atomic separation distances, ϵ is the two-body energy at $r_{ij} = r_0$ while the exponents m and n account for the repulsive and attractive two-body contributions respectively. In eq. (1c), θ_i, θ_j, θ_k and r_{ij}, r_{ik}, r_{jk} represent the angles and sides formed by three particles i, j and k while Z is the three body intensity parameter. In this general form, Φ is a function of both the material parameters ϵ, r_0, m, n, Z and the atomic configuration of the system.

Choosing $m = 12$ and $n = 6$, using unitless quantities, and lattice sums, the total reduced interaction energy for a crystalline structure, can be written from eq. (1) as

$$\Phi^* = \frac{1}{2} \left\{ A_{12}(r^*)^{12} - 2A_6(r^*)^6 \right\} + Z^* T_k (r^*)^9 \qquad (2a)$$

where the reduced quantities are defined as

$$\Phi^* = \frac{\Phi}{N\epsilon} \; ; \quad r^* = \frac{r_o}{d} \; ; \quad z^* = \frac{z}{\epsilon r_o^9} \qquad (2b)$$

and the lattice sums are

$$A_{12} = \sum_{j>1}^{N} \left(\frac{d}{r_{1j}}\right)^{12} \; ; \quad A_6 = \sum_{j>1}^{N} \left(\frac{d}{r_{1j}}\right)^{6} \; ;$$

$$T_k = \frac{1}{6} \sum_{\substack{j \ k \\ j \neq k > 1}}^{N \ N} \frac{1 + 3 \cos \theta_1 \cos \theta_j \cos \theta_k}{\left(\frac{r_1}{d} \frac{r_j}{d} \frac{r_k}{d}\right)^3} \qquad (2c)$$

with d denoting the nearest neighbor distance in the crystal. For each chosen crystal structure, the lattice sums have unique values which are listed in Table 1.

The convergence of the two body lattice sums, A_m, is rapid for large m. Computed lattice sums A_{12} and A_6 are in good agreement with the results of Bell and Zucker for the BCC, FCC and HCP structures[5]. The sum T_k is very slowly converging.

The stability condition for a crystal at T = 0°K can be obtained by considering $\partial \Phi^*/\partial v = 0$ or $\partial \Phi^*/\partial d = 0$ since the atomic volume v is related to d by $v = gd^3$ where g is a geometrical constant. Values of g are tabulated in Table 1 for various crystals. Thus, the stability condition becomes

$$A_{12}(r^*)^{12} - A_6(r^*)^6 + \frac{3}{2} z^* T_k (r^*)^9 = 0 \; . \qquad (3)$$

The surface energy, σ, per surface atom was calculated from

$$\sigma = \frac{1}{N_s} \sum_{\ell=1}^{M} (E_\ell - E_0) \qquad (4)$$

where E_ℓ is the total interaction energy for an atom located in the ℓ'th layer from the surface, E_0 is the corresponding value for a layer far inside the crystal away from any influence due to the surface, M is the total number of surface layers considered in the calculation and N_s is the total number of atoms at the expected surface. At a finite temperature, σ is expressed as the sum of two parts, σ_{un} and δ_{rel}, where σ_{un} represents the surface energy for the atoms in unrelaxed positions while δ_{rel} is the change due to relaxation given by

$$\delta_{rel} = \frac{1}{N_s} \sum_{\ell=1}^{M'} (\Delta E_\ell - \Delta E_0) . \qquad (5)$$

Throughout this investigation, relaxations for M' = 2 and T = 298°K with the remainder of the atoms fixed were performed using a Monte Carlo technique based on the Metropolis approximation[1].

RESULTS AND DISCUSSION

A. <u>Structural Stability</u>

Using eqs. (2) and (3), minimum values of Φ^*, for various crystalline structures, were calculated as a function of z^* and are shown in Figure 1. We note that the more densely packed structures are favored at small z^* and the more loosely packed structures at large z^*. The diamond cubic structure is the most stable in the range $0.55 < z^* < 0.80$. Including the

previous results of Halicioglu[4] that the HCP structure has the lowest energy without the three body interaction (i.e., for $z^* = 0$), structural stability appears to change in the following order with increasing z^*

$$HCP \rightarrow FCC \rightarrow DIA \rightarrow GRAPH . \qquad (6)$$
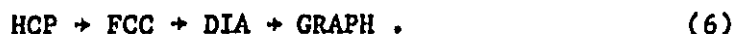
we were unable to find any region of z^* where the BCC structure is the most stable structure for $m = 12$ and $n = 6$; however, the BCC structure becomes stable for other values of m and n.

Figure 2 shows our calculated results for Φ^* as a function of atomic volume for $z^* = 0.3$ (FCC most stable), $z^* = 0.7$ (DIA most stable and $z^* = 11$ (GRAPH most stable). We note that both the minimum energy and the equilibrium volume, v^*, (volume at Φ^*_{min}) increase for all structures as z^* increases. Table 2 lists these numerical values of Φ^*_{min} and v^* for the different structures. Considerable variation of these values with z^* exists for the FCC structure but not for the graphite structure. From Fig. 2b we note that, for the stable diamond structure, if v is decreased by 14% or more (by increase of pressure) a phase transition is expected to occur to the β-tin structure. Likewise, from Fig. 2c, one may anticipate a graphite $\rightarrow$ diamond structural transition if v is decreased by 19% or more. Thus, these parameteric studies lead to the conclusion that, within the stability region of the diamond cubic or graphite structure, the diamond cubic $\rightarrow$ β-tin and the graphite $\rightarrow$ diamond cubic structural transformations may be expected upon application of sufficient external pressure.

Most group IV materials (C, Si, Ge, Sn) exhibit the diamond cubic structure and their phase diagrams show that Si, Ge and Sn tend to form the β-tin structure under high pressure. Furthermore, the stable structure for C at NTP is the graphite structure which tends to transform to the diamond cubic structure under sufficiently high pressure.

By evaluation of the elastic constants, the diamond cubic form has been shown to be absolutely stable for $z^* > 0.55$ but unstable to shear forces below this value. Thus, mechanical stability of this crystal structure requires the presence of a many-body force. This study will be published elsewhere[6].

B. Surface Energy

For the relaxation procedure, the surface and bulk energies, σ and E_0 were calculated for different z^* values ranging from 0.6 to 0.9 where the diamond cubic structure is stable. The (111), (100) and (110) surface planes were chosen for consideration and the top-most two surface layers were relaxed to minimize σ. The calculation system contained approximately 280 atoms and considered about 10 atomic layers. In Table 3, values of σ_{un}, δ_{rel} and σ are given for these three orientations in reduced units at various z^*. We note that the (111) has the lowest surface energy while the (100) has the highest and that σ decreases for all three orientations as z^* increases.

The top and side views of the (100), (110) and (111) planes with $z^* = 0.7$ after relaxation are shown in Fig. 3. For all three surfaces, the top layer exhibits a large contraction while changes in the second layer relative to the bulk spacing are very small. The surface geometry after

8

relaxation was found to be relatively insensitive to z^* value in the diamond cubic stability range. No change with relaxation was found for the top view of the (111) and (110); however, the (100) exhibited dimer formation. This reflects the relaxation energy, δ_{rel}, which Table 3 shows us is ~ 5 - 10 times larger for the (100) than either of the other surfaces. The reconstruction patterns for the (100), (110) and (111) surfaces are thus $C(2 \times 2)$, (1×1) and (1×1) respectively.

In Fig. 4, the reduced surface energy $\sigma^* = |\sigma/E_0|$ and the bulk energy, E_0, are plotted as a function of z^*. For all three orientations, σ^* was found to decrease monotonically with increase of z^*. The bulk energy, E_0, exhibits the opposite trend with increasing z^*. Experimentally, approximate values of reduced surface energy for Group IV elements (C, Si, Ge and Sn) are in the range ~ 0.14 - 0.25 and these are within the calculated range of Fig. 4.

To estimate the "relative" experimental surface energy, we take the raw data of Table 4 for lattice constant, a_0, surface energy, γ, and enthalpy of formation at 298°K, ΔH^0_{298}. Since the surface area per surface atom a is given by $0.217\ a_0^2$, $0.354\ a_0^2$ and $0.5\ a_0^2$ for the (111), (110) and (100) planes respectively, we can define the reduced surface energy by $\theta = \gamma a/\Delta H^0_{298}$. Values of θ for the major orientations and the average value $\bar{\theta}$ are given in Table 5.

CONCLUSIONS

Atomistic calculations using a two-body-only PEF are unable to predict the relative stability for FCC, BCC, diamond cubic and graphite structures; however, addition of a many-body term in the form of a three-body

contribution does allow such a prediction. The present calculations predict that the structural stability order with increasing three-body strength, z^*, is HCP → FCC → β-tin → Diamond → Graphite. In addition, structural transformations from diamond cubic → β-tin and graphite → diamond cubic are predicted to occur by increases of pressure.

Multilayer surface relaxation of the principle orientations in the diamond cubic structure shows marked contraction of the first interlayer spacing for the (100, (110) and (111) with dimer formation on the (100) and calculated surface energies, σ^*, in the expected range for the experimental values.

This study emphasises the need for inclusion of multibody forces in the PEF when dealing with both structural stability and surface energies of non-close packed structures. The PEF employed in this study was a particularly simple and useful one because it allowed ease and speed of computation in lengthy iterative procedures.

REFERENCES

1. G.C. Maitland, M. Rigby, E.B. Smith and W.A. Wakeham, _Intermolecular Forces: Their Origin and Determination_ (Clarendon Press, Oxford, 1981).

2. T. Halicioglu and P.J. White, J. Vac. Sci., Technol. $\underline{17}$, 1213 (1980) and Surf Sci. $\underline{106}$, 45 (1981).

3. T. Halicioglu, H.O. Pamuk and S. Erkoc, Surf. Sci. $\underline{143}$, 601 (1984).

4. T. Halicioglu, Phys. Stat. Sol. (b) $\underline{99}$, 347 (1980).

5. R.J. Bell and I.J. Zucker in _Rare Gas Solids_, Eds. M.L. Klein and J.A. Venables (Academic Press, New York, 1976), p. 123.

6. T. Takai, T. Halicioglu and W.A. Tiller, to be published.

7. R.W.G. Wyckoff, _Crystal Structure_, 2nd edition (John Wiley & Sons, New York, 1963) Vol. 1.

8. B.N. Oshcherim, Phys. Stat. Sol. (a) $\underline{34}$, K181 (1976).

9. H. Wawra, Z. Metallkde $\underline{66}$, 395 (1975).

10. _JANAF Theromechemical Tables_, 2nd edition, 1971. NSRDS-NBS37, U.S. Department of Commerce, National Bureau of Standards.

11. I. Barin and O. Knakke, _Thermochemical Properties of Inorganic Substances_ (Springer-Verlag, New York, 1973).

12. C. Kittel, _Introduction to Solid State Physics_, 5th edition (John Wiley & Sons, New York, 1976).

Table 1

Lattice Sums for the Mie and Axilrod-Teller Potentials
Plus the Geometrical Constant, g, for Various Structures

	FCC	BCC	DIA	GRAPH	?-tin
A_6	14.4481	12.2495	5.1153	3.3895	8.2864
A_{12}	12.1319	9.1141	4.0389	3.0092	5.4654
T_k	19.1697	14.7719	1.6647	0.1010	7.0706
$g^{\#}$	0.70711	0.7698	1.5396	3.067	0.9797
$\#^{\dagger}$	6912	8192	5832	5040	7200

† indicates the number of atoms which were considered to
compute the lattice sums.

$\#g = v/d^3$.

Table 2

The minimum energies, Φ^*_{min}, and the equilibrium volume, v^*, for five different structures as a function of z^*.[†]

z^*	ϕ^*_{min}/v^*	FC	BCC	Diamond	Graphite	β-tin
0.3	Φ^*_{min}	−3.8212	−3.7494	−2.6086	−1.8731	−3.4417
	v^*	0.8925	0.9051	1.4854	2.9105	1.0057
0.7	Φ^*_{min}	−1.5849	−1.5871	−1.9763	−1.8265	−1.7145
	v^*	1.3065	1.3116	1.6562	2.9382	1.3475
1.1	Φ^*_{min}	−0.8073	−0.8165	−1.5188	−1.7812	−0.9640
	v^*	1.7835	1.7806	1.8425	2.9662	1.7426

† All values are reduced according to eq. (2).

Table 3

Calculated surface energies of the low index planes
for the diamond cubic structure at several different Z^* values.

Z^*		(100)	(110)	(111)
0.6	σ_{un}	0.8266	0.4374	0.2084
	δ_{rel}	-0.3624	-0.0298	-0.014
	σ	0.4342	0.4076	0.1944
0.7	σ_m	0.7426	0.3630	0.1696
	δ_{rel}	-0.3714	-0.0492	-0.0292
	σ	0.3712	0.3138	0.1404
0.8	σ_m	0.6672	0.2978	0.1362
	δ_{rel}	-0.3872	-0.075	-0.0406
	σ	0.2800	0.2228	0.0956
0.9	σ_m	0.6010	0.2414	0.107
	δ_{rel}	-0.4152	-0.1114	-0.1006
	σ	0.1854	0.130	0.0065
Total number of atoms in the system		216	360	288
Total number of atoms on the surface		18	30	48

Table 4

Group IV experimental data for lattice constant, a_0, surface energy, γ, and bulk energy, ΔH_{298}^0

Element	a_0(Å)	γ(ergs/cm^2)	ΔH_{298}^0(eV/atom)
C$_{\text{diamond}}$	3.5668[7]	3760.0[8]	7.412[10,11]
Si	5.4307[7]	1389.0[9]	4.673[10,11]
Ge	5.6574[7]	975.5[9]	3.85[12]
Sn	6.4912[7]	822.0[9]	3.14[12]

Table 5

Reduced surface tension, θ, for Group IV elements

Species	$a_{(111)}(cm^2)$ $\gamma^\circ a_{(111)}(eV)$	$a_{(110)}(cm^2)$ $\gamma^\circ a_{(110)}(eV)$	$a_{(100)}(cm^2)$ $\gamma^a a_{(100)}(eV)$	$\theta_{(111)}$	$\theta_{(110)}$	$\theta_{(100)}$	$\bar{\theta}$
$C_{diamond}$	2.7544×10^{-16}	4.4979×10^{-16}	6.3610×10^{-16}	0.0873	0.1426	0.20167	0.1439
	0.6472	1.057	1.4948				
Si	6.3853×10^{-16}	1.0427×10^{-15}	1.4746×10^{-15}	0.11862	0.1937	0.2739	0.1954
	0.55432	0.90519	1.28014				
Ge	6.9295×10^{-16}	1.13157×10^{-15}	1.600×10^{-15}	0.10974	0.17919	0.2534	0.18077
	0.42248	0.6899	0.9755				
Sn	9.1226×10^{-16}	1.4897×10^{-15}	2.1068×10^{-15}	0.1493	0.2437	0.3447	0.2459
	0.46867	0.76533	1.08237				

FIGURE CAPTIONS

1. The minimum reduced energy, Φ^*, for FCC, BCC, diamond cubic (DIA) and graphite (GRAH) structure as a function of the reduced three-body parameter, z^*, (m = 12, n = 6).

2. The reduced energy, Φ^*, as a function of the atomic volume, V, for FCC, BCC, DIA, GRAH and β-tin structures (m - 12, n = 6):

   (a) for z^* = 0.3, within the stability region of FCC,

   (b) for z^* = 0.7, within the stability region for DIA, and

   (c) for z^* = 1.1, within the stability region for GRAH.

3. Surface geometries (top and side views) of (a) (100), (b) (110), and (c) (111) surfaces for the diamond cubic structure after multilayer relaxation with z^* = 0.7 and Monte Carlo temperature of 298°K. The numbers below the figures indicate the percent changes in interlayer spacing.

4. Plot of the reduced surface energy, σ^*, for three different surfaces and the bulk energy E_0 on a per atom basis in the DIA system as a function of z^* at T = 298°K.
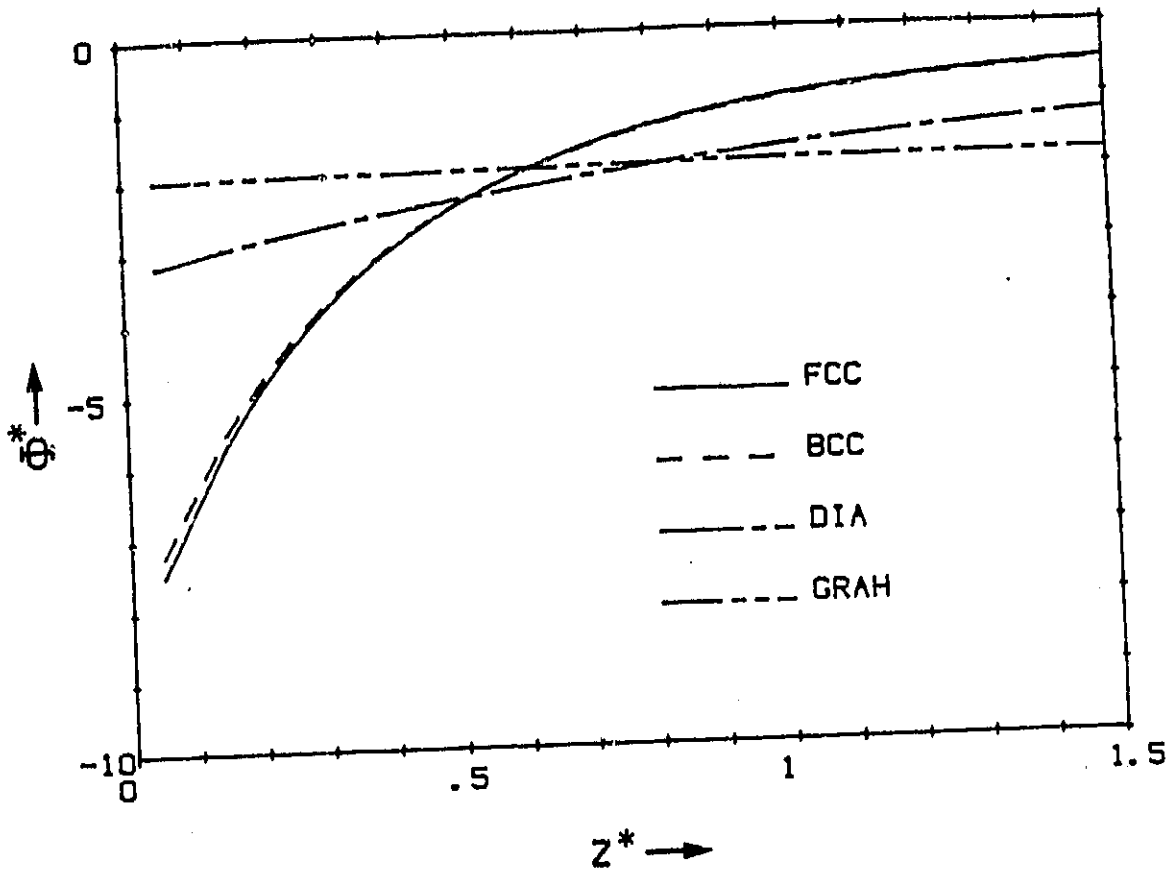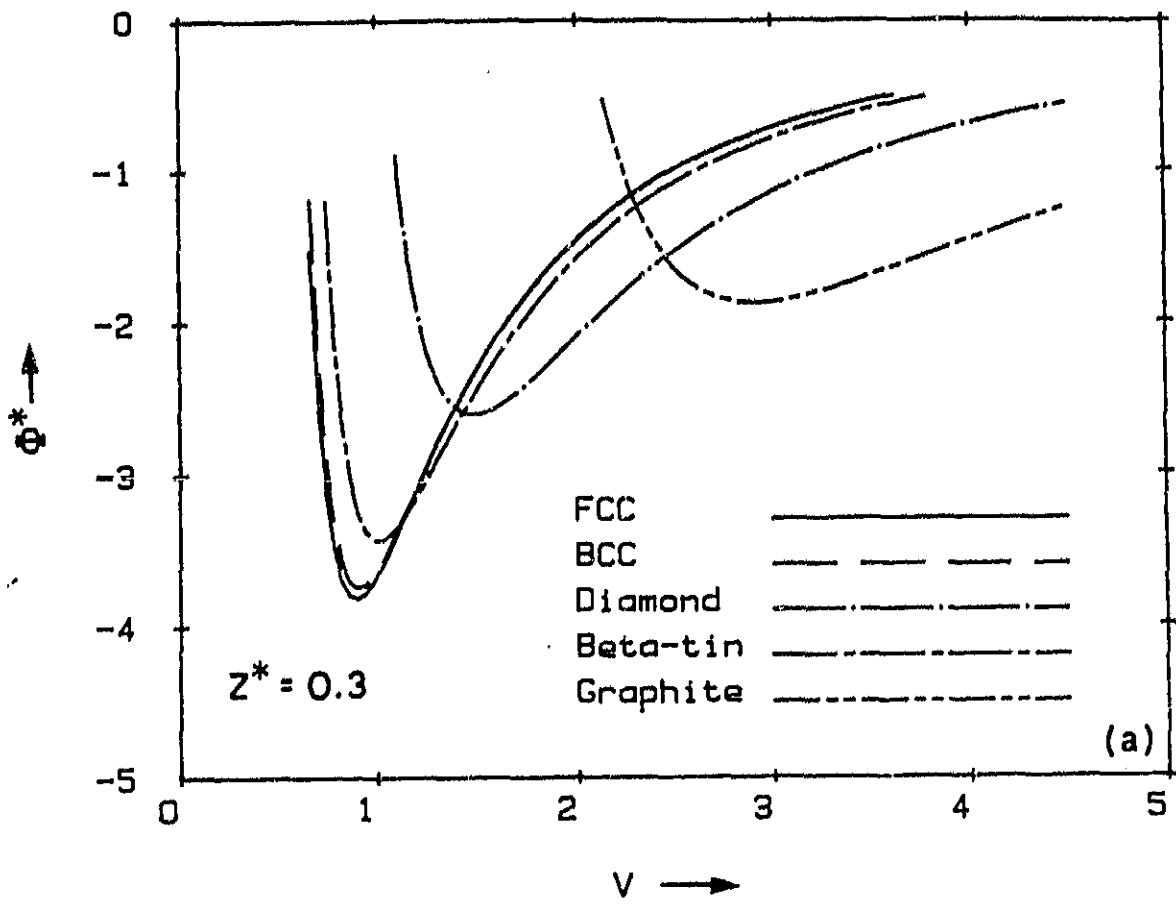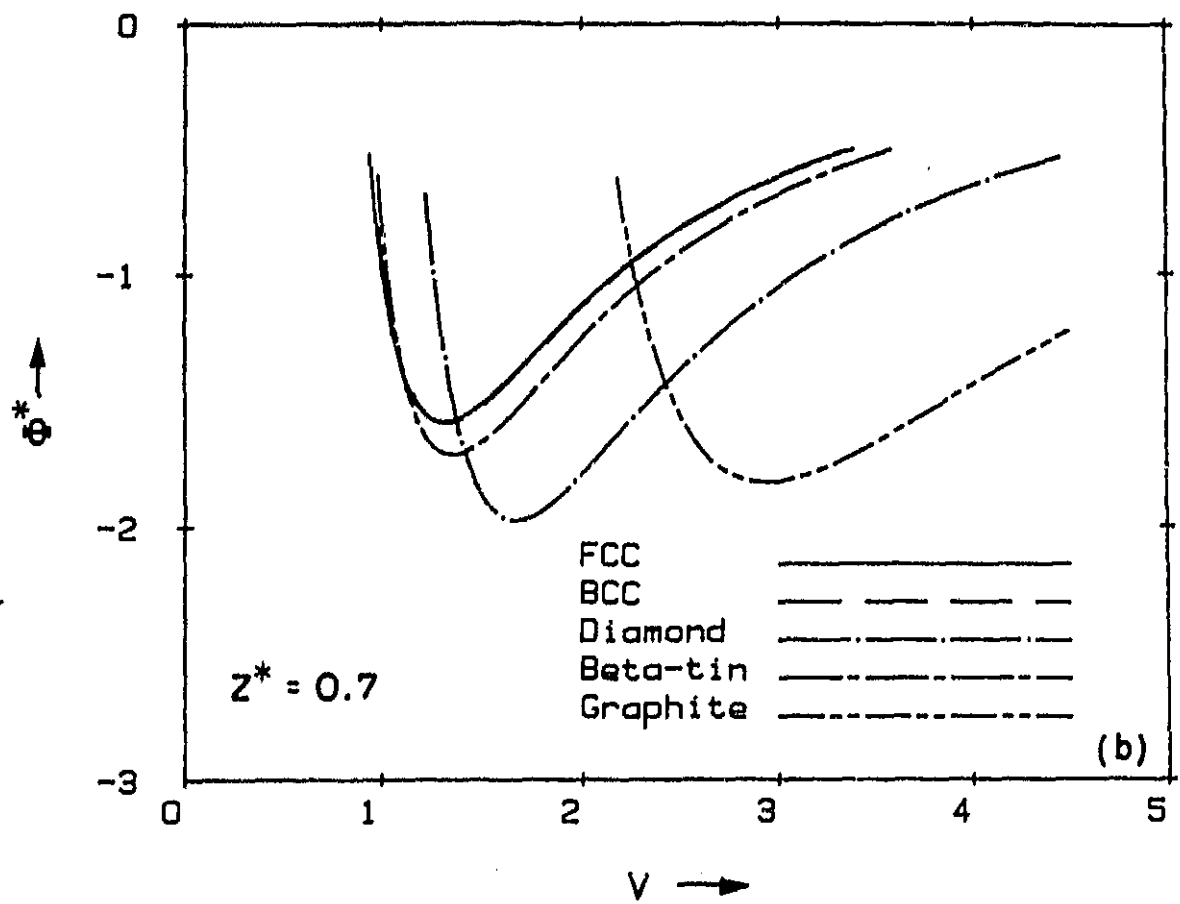
FIGURE 1

FIGURE 2a

FIGURE 2b

FIGURE 2c

- 21 -

FIGURE 3

$\Delta d_1'' = -27.2 \; (\%) \quad \Delta d_1' = 1.6 \; (\%)$
$\Delta d_2'' = 1.5 \quad (\%) \quad \Delta d_2' \approx 0.0 \; (\%)$

(c)

$\Delta d_1 = -5.8 \; (\%)$
$\Delta d_2 \approx 0.0 \quad (\%)$
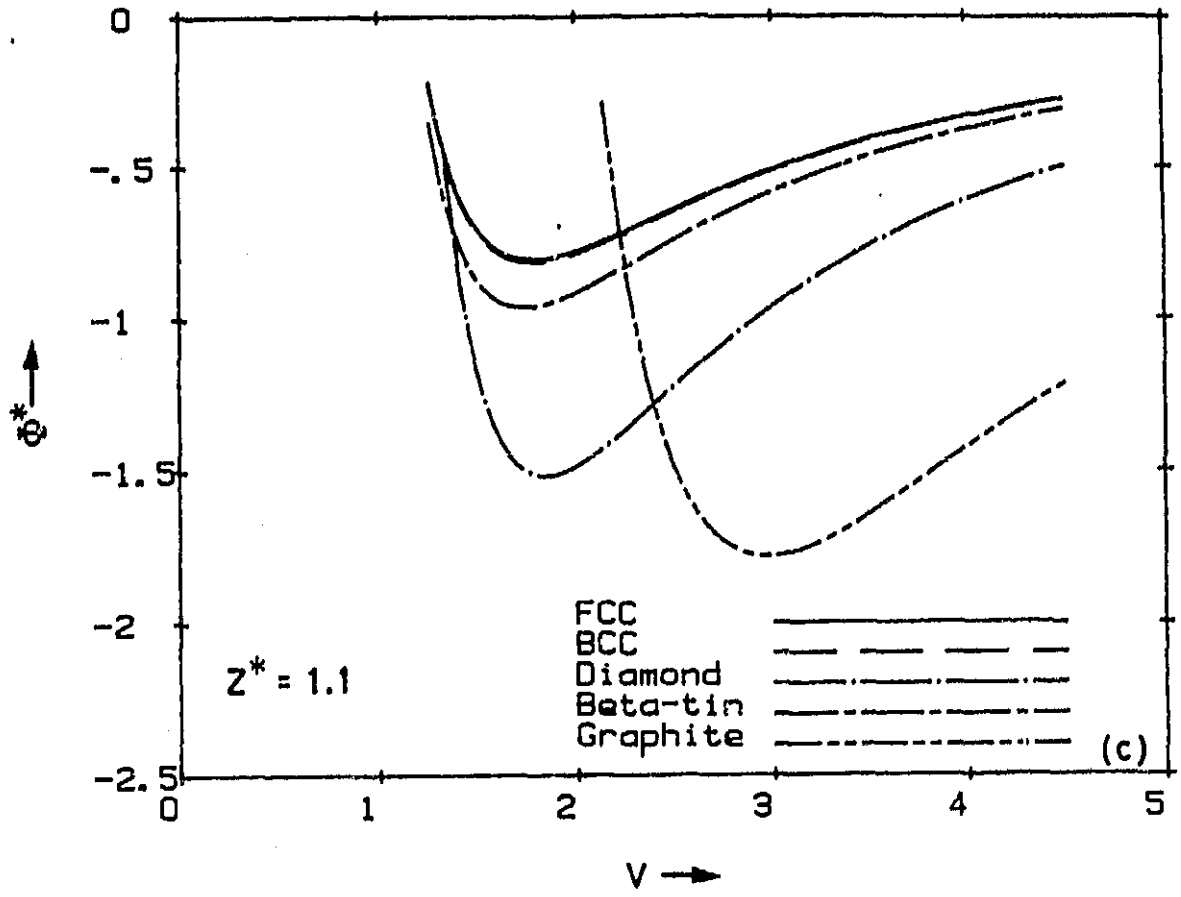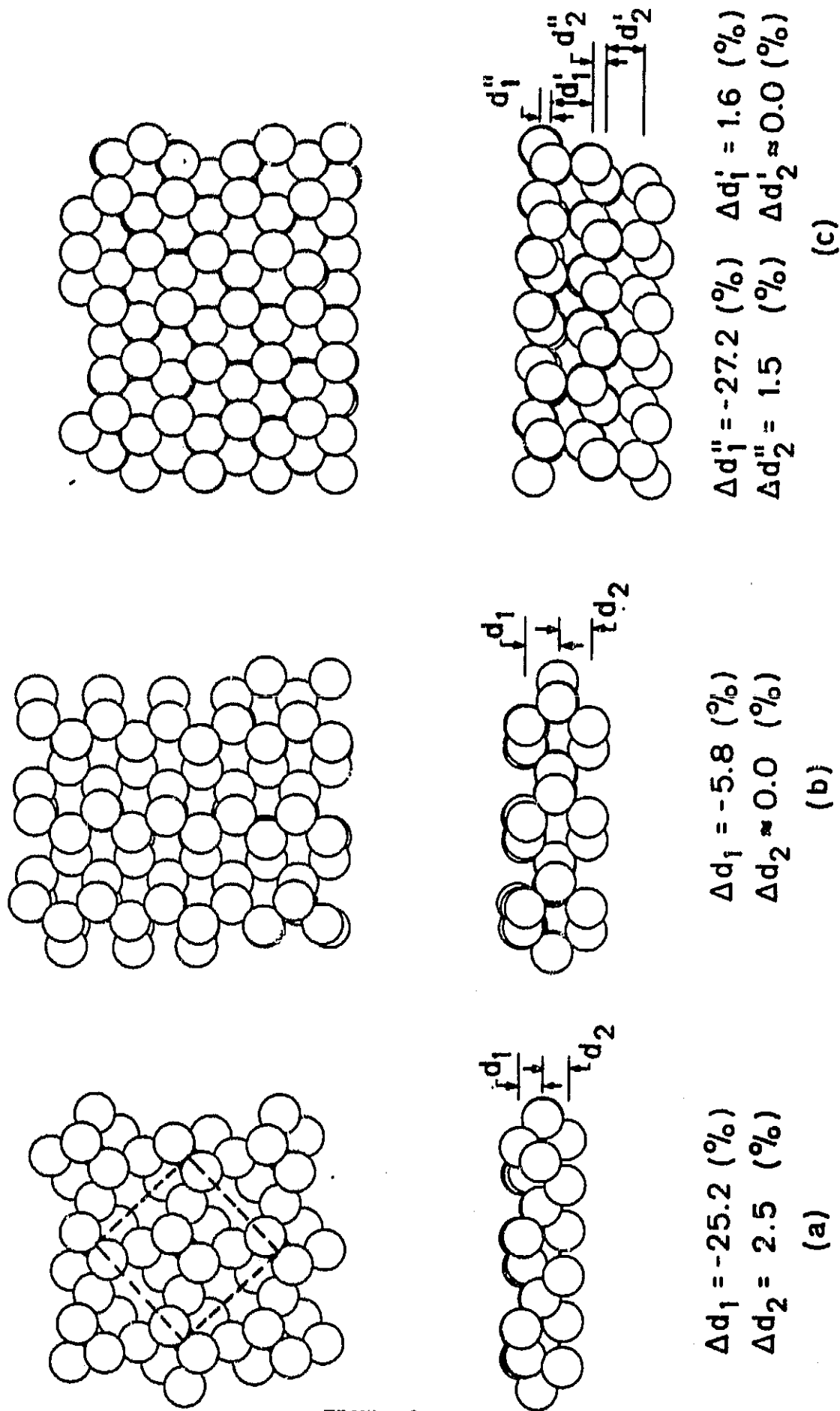
(b)

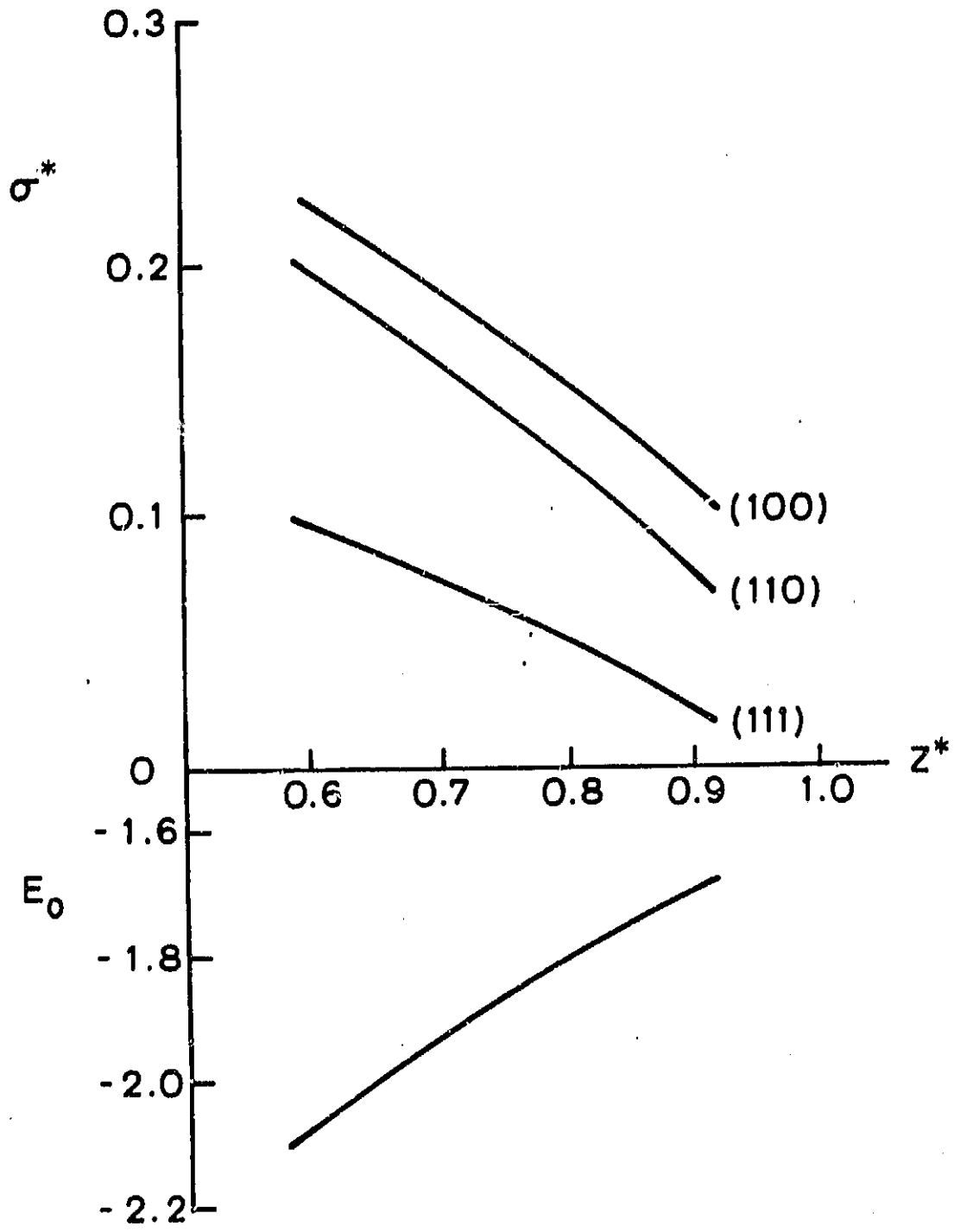$\Delta d_1 = -25.2 \; (\%)$
$\Delta d_2 = 2.5 \quad (\%)$

(a)

FIGURE 4

Chapter II

ABSOLUTE CRYSTAL STABILITY AND ELASTIC CONSTANTS FOR CUBIC STRUCTUTRES

INTRODUCTION

In a previous paper, the relative stability of various open crystal structures was shown to require a multi-body potential interaction in addition to the usual two-body interaction.[1] There, the multi-body term was chosen to be a simple three-body potential and a parametric analysis was used. In the present work, this analysis is extended to examine the mechanical stability of various cubic structures against all types of homogeneous elastic deformations. As a necessary precursor, a parametric analysis of the elastic constants is obtained.

Using unitless quantities, a two-body Mie potential, a three-body Axilrod-Teller potential and lattice sums of the energy, the total reduced interaction energy, Φ^*, for an atom in a particular crystalline structure was shown to be given by[1]

$$\Phi^* = \frac{1}{2(m-n)} \left\{ nA(r^*)^m - mB(r^*)^n \right\} + z^* T_k (r^*)^9 \qquad (1a)$$

with

$$\Phi^* = \frac{\Phi}{N\epsilon} \ , \ r^* = \frac{r_o}{d} \ , \ z^* = \frac{z}{\epsilon r_o^9} \qquad (1b)$$

and

$$A = \sum_{j>1}^{N} \left(\frac{d}{r_{1j}}\right)^m , \ B = \sum_{j>1}^{N} \left(\frac{d}{r_{1j}}\right)^n ,$$

$$T_k = \frac{1}{3} \sum_{\substack{i \ j \\ i>j>1}}^{N} \sum^{N} \frac{(1 + 3 \cos \theta_1 \cos \theta_1 \cos \theta_j) \, d^9}{(r_{1i} \, r_{1j} \, r_{ij})^3} \ . \qquad (1c)$$

25

Here, m, n, c and r_o are the usual two-body parameters while Z is the three-body intensity parameter and d is the nearest neighbor distance in the crystal. For each chosen crystal structure, the lattice sums, A, B and T_k in eqs. (1) have unique values and their computed values are listed in Table 1 for the various cubic structures of interest to us in this paper.

The equilibrium nearest neighbor distance, d_o, at $T = 0°K$ may be found from eqs. (1) by requiring that the total energy be a minimum with respect to the nearest neighbor distance, d. As found earlier[1], the equilibrium equation is then written as

$$A(r^*)^m - B(r^*)^n + 18 \frac{(m-n)}{mn} Z^* T_k(r^*)^9 = 0 . \qquad (2)$$

Using eqs. (1) and (2) plus elasticity theory, the elastic constants, mechanical stability conditions and the absolute stability conditions for various crystal structures using this parametric potential may be obtained.

ELASTIC CONSTANTS

In any study of mechanical crystal stability the elastic constants are an essential quantity.[2] They may be calculated by applying a homogeneous deformation to the crystal and comparing the stored energy change with that predicted by linear continuum elasticity theory. In this procedure, the position of the i'th atom is denoted by $\vec{R}_i$ in the final configuration. According to Wallace[3], the change in distance between any two atoms in a crystal under homogeneous strain can be represented using Fig. 1 by

26

$$\sum_{\alpha} (x_1^{\alpha})^2 = \sum_{\alpha} (x_1^{\alpha})^2 + 2 \sum_{\alpha} \sum_{\beta} \eta_{\alpha\beta} \, x_1^{\alpha} \, x_1^{\beta} , \qquad (3)$$

where the indices α, β represent Cartesian coordinates and take on the values x, y, z or 1, 2, 3, and the $\eta_{\alpha\beta}$ are the Lagrangian strain parameters.

The elastic constants at $0°K$ are defined as

$$C_{\alpha\beta\gamma\delta} = \frac{1}{V} \left(\frac{\partial^2 \Phi}{\partial \eta_{\alpha\beta} \, \partial \eta_{\gamma\delta}} \right)_{\eta'} , \qquad (4)$$

where V denotes the volume of the crystal. These elastic constants are calculated at the initial configuration, $\vec{r}_1$, with the strain $\eta_{\alpha\beta}$ being measured from $\vec{r}_1$ and the derivatives all being evaluated at $\vec{r}_1$, i.e., at $\eta_{\alpha\beta} = 0$. Using eqs. (1) and (4), the reduced elastic constants may be written, using $C^*_{\alpha\beta\gamma\delta} = (V/N\epsilon) \, C_{\alpha\beta\gamma\delta}$, as

$$C^*_{\alpha\beta\gamma\delta} = \frac{mn}{4(m-n)} \left(\frac{m}{2} + 1\right) A_{\alpha\beta\gamma\delta}(r^*)^m - \frac{mn}{4(m-n)} \left(\frac{n}{2} + 1\right) B_{\alpha\beta\gamma\delta}(r^*)^n$$

$$+ z^* T_{\alpha\beta\gamma\delta}(r^*)^9 . \qquad (5)$$

The lattice sums for the elastic constants, $A_{\alpha\beta\gamma\delta}$, $B_{\alpha\beta\gamma\delta}$ and $T_{\alpha\beta\gamma\delta}$, are developed in Appendix I, have been computed and are listed in Table 2 for various cubic structures.

There are 81 elements in the matrix $[C^*_{\alpha\beta\gamma\delta}]$ and, considering the strain and crystalline symmetries plus using the Voigt notation[4], the matrix of elastic constants for the cubic system becomes

$$
[C^*_{pq}] =
\begin{bmatrix}
C^*_{11} & C^*_{12} & C^*_{12} & & & \\
C^*_{12} & C^*_{11} & C^*_{12} & & 0 & \\
C^*_{12} & C^*_{12} & C^*_{11} & & & \\
& & & C^*_{44} & 0 & 0 \\
& 0 & & 0 & C^*_{44} & 0 \\
& & & 0 & 0 & C^*_{44}
\end{bmatrix}
\tag{6}
$$

In Eq. (6), there are three independent elastic constants; i.e, C^*_{11}, C^*_{12} and C^*_{44}. It is well known that the Cauchy relations, $C_{12} = C_{44}$ for the cubic system, hold if each pair of atoms interact through a purely central potential[5]. This relationship can be seen in Table 2 for the two-body part of the lattice sums for the elastic constants, i.e.; $A_{12} = A_{44}$ and $B_{12} = B_{44}$. Of course, it does not hold for the three-body portion which is not a central potential.

Using eqs. (2) and (5) with $m = 12$ and $n = 6$, the elastic constants C^*_{pq} for the FCC, BCC, diamond cubic and simple cubic crystal structures have been calculated as a function of z^* and are shown in Figs. 2. Except for the C_{12} and C_{44} of the simple cubic structure, all the elastic constants, (C_{11}, C_{12}, C_{44}), decrease as z^* increases.

ABSOLUTE CRYSTAL STABILITY

For a crystal to be stable against all elastic homogeneous deforma-tions, the elastic strain energy, $\frac{1}{2} C_{\alpha\beta\gamma\delta} \eta_{\alpha\beta} \eta_{\gamma\delta}$, must be positive. This condition requires that the matrix of elastic constants, $[C_{pq}^{*}]$, be positive definite; i.e., all eigenvalues of the matrix $[C_{pq}^{*}]$ are positive.[4] Thus, the condition for mechanical stability in the cubic system is

$$C_{11} > 0; \quad C_{11} > |C_{12}|; \quad C_{44} > 0; \quad C_{11} + 2C_{12} > 0 . \qquad (7)$$

Calculated values of $C_{11} - |C_{12}|$ and $(C_{11} + 2C_{12})/3$ for each structure have been plotted in Fig. 2 to assess the mechanical stability condition via eq. (7).

For the FCC structure, a value of $z^{*} < 0.5$ satisfies the stability condition giving an extended domain of absolute stability. We note that this potential function gives no region of mechanical stability for the BCC structure although in another study[6] it was found that altering m and n led to a stability domain for the BCC structure. We note also that, without the three-body potential $(z^{*} = 0)$, the diamond cubic and simple cubic structures are not stable. However, increasing the three-body intensity parameter, z^{*}, to values greater than $z^{*} \sim 0.5$, one can stabilize the diamond cubic structure. For the simple cubic structure, the elastic constants satisfy all the stability requirements for z^{*} values in the range $0.45 < z^{*} < 0.73$.

Using eqs. (1) and (2) and Figs. 2, both the thermodynamic stability condition (minimum value of Φ^*) and the mechanical stability condition may be compared so that the domain of z^* providing absolute stability for each cubic structure may be determined. These results are shown in Fig. 3. From Fig. 3, we note that the FCC structure is absolutely stable in the range $0 < z^* < 0.45$, the BCC structure has no region of absolute stability, the simple cubic structure is absolutely stable in the range $0.45 < z^* < 0.57$ and the diamond cubic structure is absolutely stable in the range $z^* > 0.57$. Of course, these ranges of absolute stability depend on the choice of crystal structures used in the comparison and upon the type of two-body and three-body potentials used in the potential energy function. The use of different exponents (m and n) in the two-body potential are known to influence the magnitude of $\Phi^{*(7)}$ but their variation has not been analyzed in the present investigation.

CONCLUSIONS

Atomistic models based on two-body-only interactions ($z^* = 0$) cannot be used to simulate the various properties of open structures like the diamond cubic structure because this structure is not mechanically stable under such conditions. Multi-body interactions, or at least three-body interactions, are absolutely necessary to provide both thermodynamic and mechanical stability for such open structures. The domain of absolute stability for each crystal structure can be found for a chosen potential energy function and chosen list of comparison structures.

Table 1

Lattice Sums of the Energy for Mie and Axilrod-Teller potentials ($m = 12$ and $n = 6$)

	FCC	BCC	DIA[*]	SC[**]
B	14.4481	12.2495	5.1153	8.3994
A	12.1319	9.1141	4.0389	6.2021
T_k	19.1697	14.7719	1.6647	6.6138

[*] ~ Diamond cubic structure.
[**] ~ Simple cubic structure.

Table 2

Lattice Sums of Elastic Constants for FCC, BCC, Simple Cubic (SC)
and Diamond Cubic (DIA) Structures (m = 12, n = 6).

Structure	$A_{11}(A_{1111})$ $A_{12}(A_{1122})$ $A_{44}(A_{2323})$ A_{pq}(others)	$B_{11}(B_{1111})$ $B_{12}(B_{1122})$ $B_{44}(B_{2323})$ B_{pq}(others)	$T_{11}(T_{1111})$ $T_{12}(T_{1122})$ $T_{44}(T_{2323})$ T_{pq}(others)
FCC	8.1510	10.1074	274.7199
	4.0124	4.4705	172.4297
	4.0124	4.4705	57.0059
	0.0	0.0	0.0
BCC	5.0125	8.1746	222.0875
	3.5698	4.0279	129.8891
	3.5698	4.0279	40.4850
	0.0	0.0	0.0
SC	8.1337	9.6340	96.4657
	0.0679	0.7563	59.9206
	0.0679	0.7563	20.9476
	0.0	0.0	0.0
DIA	1.8050	2.6088	26.0069
	1.7899	2.0955	14.1703
	1.7899	2.0955	9.2187
	0.0	0.0	0.0

REFERENCES

1. See Chapter I.

2. Z.S. Basinski, M.S. Duesbery, A.P. Pogany, R. Taylor and Y.P. Varshni, Can. J. Phs. 48, 1480 (1970).

3. D.C. Wallace, "Thermodynamics of Crystals", (John Wiley & Sons, New York, 1972).

4. J.F. Ney, "Physical Properties of Crystals", (Oxford, 1972).

5. H.B. Huntington, "The Elastic Constants of Crystals", (Academic Press, New York, 1958).

6. T. Halicioglu, Phys. Stat. Sol. (b) 99, 347 (1980).

7. T. Takai, "Computer Simulation of Silicon, Carbon, Silicon Carbide and Gold: Surface Processes and Energetics", Ph.D. Thesis, Stanford University, December 1984.

Lattice Sum Formulae for Elastic Constants Using Mie Potential (two-body) and Axilrod-Teller Potential (three-body) Terms

Defining our potential, Φ, as the sum of a two-body, Φ_2, and a three-body, Φ_3, term, the two-body part can be written as

$$\Phi_2 = \frac{N\epsilon}{2} \sum_{i=1}^{N} \left\{ \frac{n}{m-n} \left(\frac{r_o^2}{r_i^2}\right)^{m/2} - \frac{m}{m-n} \left(\frac{r_o^2}{r_i^2}\right)^{n/2} \right\} . \tag{I-1}$$

Let us define

$$X_0 = r_o^2 \; ; \quad X_1 = r_i^2 \; ; \quad \phi_2 = \frac{n}{m-n} \left(\frac{x_0}{x_1}\right)^{m/2} - \frac{m}{m-n} \left(\frac{x_0}{x_1}\right)^{n/2} , \tag{I-2}$$

then we have

$$\frac{\partial^2 \Phi_2}{\partial \eta_{\alpha\beta} \partial \eta_{\gamma\delta}} = \frac{N\epsilon}{2} \sum_{i=1}^{N} \frac{\partial^2 \phi_2}{\partial x_i^2} \frac{\partial X_1}{\partial \eta_{\alpha\beta}} \frac{\partial X_1}{\partial \eta_{\gamma\delta}} \tag{I-3a}$$

$$= \frac{N\epsilon}{2} \frac{mn}{2(m-n)} \left\{ (\frac{m}{2} + 1)(\frac{r_o}{d})^m A_{\alpha\beta\gamma\delta} - (\frac{n}{2} + 1)(\frac{r_o}{d})^n B_{\alpha\beta\gamma\delta} \right\} \tag{I-3b}$$

where the two-body lattice sums $A_{\alpha\beta\gamma\delta}$ and $B_{\alpha\beta\gamma\delta}$ are given by

$$A_{\alpha\beta\gamma\delta} = \sum_{i=2}^{N} \left(\frac{d}{r_{1i}}\right)^m \frac{4x_i^\alpha x_i^\beta x_i^\gamma x_i^\delta}{r_{1i}^4} \tag{I-4a}$$

$$B_{\alpha\beta\gamma\delta} = \sum_{i=2}^{N} \left(\frac{d}{r_{1i}}\right)^n \frac{4x_i^\alpha x_i^\beta x_i^\gamma x_i^\delta}{r_{1i}^4} \qquad \text{(I-4b)}$$

and $2x_i^p x_i^q = \partial X_i/\partial\eta_{pq}$.

The three-body part of the potential, Φ_3, is given by

$$\Phi_3 = \frac{N}{3!} Z_1 \sum_{\substack{i \\ i \neq j}}^{N} \sum_{j}^{N} \frac{1 + 3\cos\theta_i \cos\theta_j \cos\theta_1}{(r_{1i}\, r_{1j}\, r_{ij})^3} \qquad \text{(I-5a)}$$

$$= \frac{N}{3!} Z_1 \sum_{\substack{i \\ i \neq j}}^{N} \sum_{j}^{N} \left\{ \frac{1}{(r_{1i} r_{1j} r_{ij})^3} + \frac{3}{8} \frac{(r_{1i}^2 + r_{1j}^2 - r_{ij}^2)(r_{1i}^2 + r_{ij}^2 - r_{1j}^2)(r_{1j}^2 + r_{ij}^2 - r_{1i}^2)}{(r_{1i}^2 + r_{1j}^2 - r_{ij}^2)^5} \right\}$$
$$\text{(I-5b)}$$

from Fig. 1.

Let us define $X = r_{1i}^2$, $Y = r_{1j}^2$ and $Z = r_{ij}^2$ and ϕ_3 as

$$\phi_3 = \frac{1}{(XYZ)^{3/2}} + \frac{3}{8} \frac{(X+Y-Z)\,(X+Z-Y)\,(Y+Z-X)}{(XYZ)^{5/2}} \quad . \qquad \text{(I-6)}$$

Then, the three-body lattice sums in the elastic constants can be written as

$$T_{\alpha\beta\gamma\delta} = \frac{1}{6} d^9 \sum_{\substack{i \\ i \neq j}}^{N} \sum_{j}^{N} (\tilde{e}_1^T \tilde{D}_3 \tilde{e}_2) \qquad \text{(I-7a)}$$

where $\tilde{e}_1$ and $\tilde{e}_2$ are the column vectors, $\tilde{D}_3$ is the (3×3) matrix and these have the following elements

$$\tilde{e}_1^T = \left(\frac{\partial X}{\partial \eta_{\alpha\beta}}, \frac{\partial Y}{\partial \eta_{\alpha\beta}}, \frac{\partial Z}{\partial \eta_{\alpha\beta}}\right) ; \quad \tilde{e}_2^T = \left(\frac{\partial X}{\partial \eta_{\gamma\delta}}, \frac{\partial Y}{\partial \eta_{\gamma\delta}}, \frac{\partial Z}{\partial \eta_{\gamma\delta}}\right)$$

$$\tilde{D}_3 = \begin{bmatrix} \dfrac{\partial^2 \phi_3}{\partial X^2} & \dfrac{\partial^2 \phi_3}{\partial X \partial Y} & \dfrac{\partial^2 \phi_3}{\partial X \partial Z} \\[2ex] \dfrac{\partial^2 \phi_3}{\partial Y \partial X} & \dfrac{\partial^2 \phi_3}{\partial Y^2} & \dfrac{\partial^2 \phi_3}{\partial Y \partial Z} \\[2ex] \dfrac{\partial^2 \phi_3}{\partial Z \partial X} & \dfrac{\partial^2 \phi_3}{\partial Z \partial Y} & \dfrac{\partial^2 \phi_3}{\partial Z^2} \end{bmatrix} . \qquad \text{(I-7b)}$$

The elements in eq. (I-7b) can also be written using atomic coordinates:

$$\frac{\partial X}{\partial \eta_{\alpha\beta}} = 2x_i^\alpha x_i^\beta ; \quad \frac{\partial Y}{\partial \eta_{\alpha\beta}} = 2x_j^\alpha x_j^\beta ; \quad \frac{\partial Z}{\partial \eta_{\alpha\beta}} = 2(x_i^\alpha - x_j^\alpha)(x_i^\beta - x_j^\beta) \qquad \text{(I-8a)}$$

and

$$\frac{\partial^2 \phi_3}{\partial X^2} = f(X,Y,Z) ; \quad \frac{\partial^2 \phi_3}{\partial Y^2} = f(Y,Z,X) ; \quad \frac{\partial^2 \phi_3}{\partial Z^2} = f(Z,X,Y) ,$$

$$\frac{\partial^2 \phi_3}{\partial X \partial Y} = \frac{\partial^2 \phi_3}{\partial Y \partial X} = g(X,Y,Z) ; \quad \frac{\partial^2 \phi_3}{\partial X \partial Z} = \frac{\partial^2 \phi_3}{\partial Z \partial X} = g(Z,X,Y) ,$$

$$\frac{\partial^2 \phi_3}{\partial Y \partial Z} = \frac{\partial^2 \phi_3}{\partial Z \partial Y} = g(Y,Z,X) , \qquad \text{(I-8b)}$$

where $f(X,Y,Z)$ and $g(X,Y,Z)$ are defined as

$$f(X,Y,Z) = \frac{15}{4(XYZ)^{3/2}} \frac{1}{X^2} + \frac{3}{8(XYZ)^{5/2}} \left[2(Y+Z-X) - 2(X+Z-Y) - 2(X+Y-Z) \right.$$

$$+ \frac{5}{X} \left\{ (X+Y-Z)(X+Z-Y) - (X+Z-Y)(Y+Z-X) - (X+Y-Z)(Y+Z-X) \right\}$$

$$\left. + \frac{35}{4X^2} \left\{ (X+Y-Z)(X+Z-Y)(Y+Z-X) \right\} \right] , \tag{I-8c}$$

and

$$g(X,Y,Z) = \frac{9}{4(XYZ)^{3/2}} \frac{1}{XY} + \frac{3}{8(XYZ)^{5/2}} \left[2(X+Y-Z) + \frac{5}{2}(X+Z-Y)(Y+Z-X)(-\frac{1}{X} - \frac{1}{Y}) \right.$$

$$+ \frac{5}{2}(X+Y-Z)(Y+Z-X)(\frac{1}{X} - \frac{1}{Y}) + \frac{5}{2}(X+Y-Z)(X+Z-Y)(-\frac{1}{X} + \frac{1}{Y})$$

$$\left. + \frac{25}{4XY}(X+Y-Z)(X+Z-Y)(Y+Z-X) \right] . \tag{I-8d}$$

Using eqs. (7) and (8), the three-body lattice sums for the various crystal structures were calculated and listed in Table 2.

FIGURE CAPTIONS

1. Atom geometry needed in the evaluation of strain parameters and the lattice sums of the elastic constants.

2. Variation of the elastic constants (C_{11}, C_{12}, C_{44}), $C_{11} - |C_{12}|$ and $(C_{11} + 2C_{12})/3$ as a function of z^* for (a) FCC, (b) BCC, (c) Diamond Cubic, and (d) Simple Cubic structures.

3. Reduced energy, ϕ^*, for the FCC, BCC, Diamond Cubic (DIA) and Simple Cubic (SC) structures as a function of z^*, plus mechanical stability regions for FCC, BCC, DIA and SC structures based on their elastic constants.
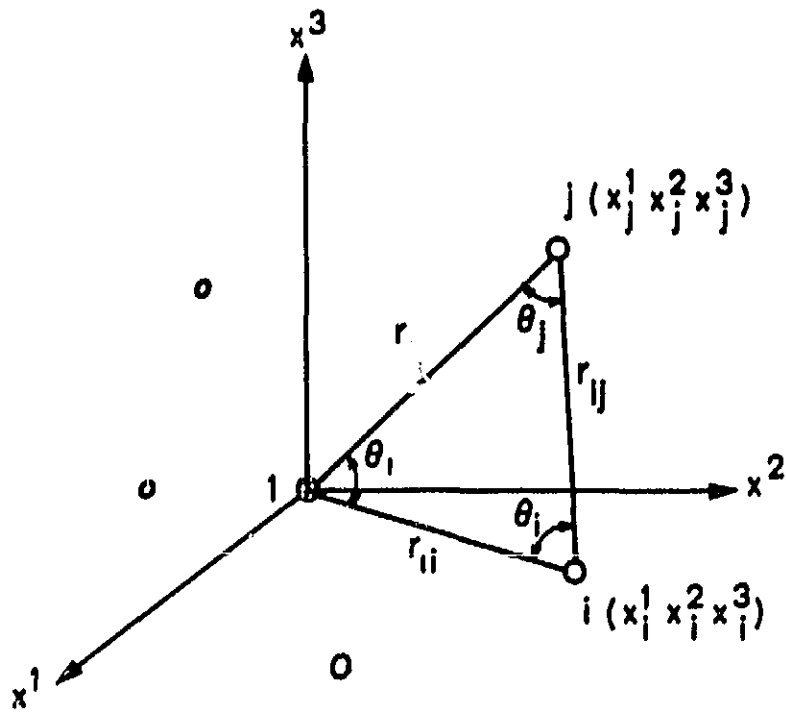
x^3

$j\,(x_j^1\,x_j^2\,x_j^3)$
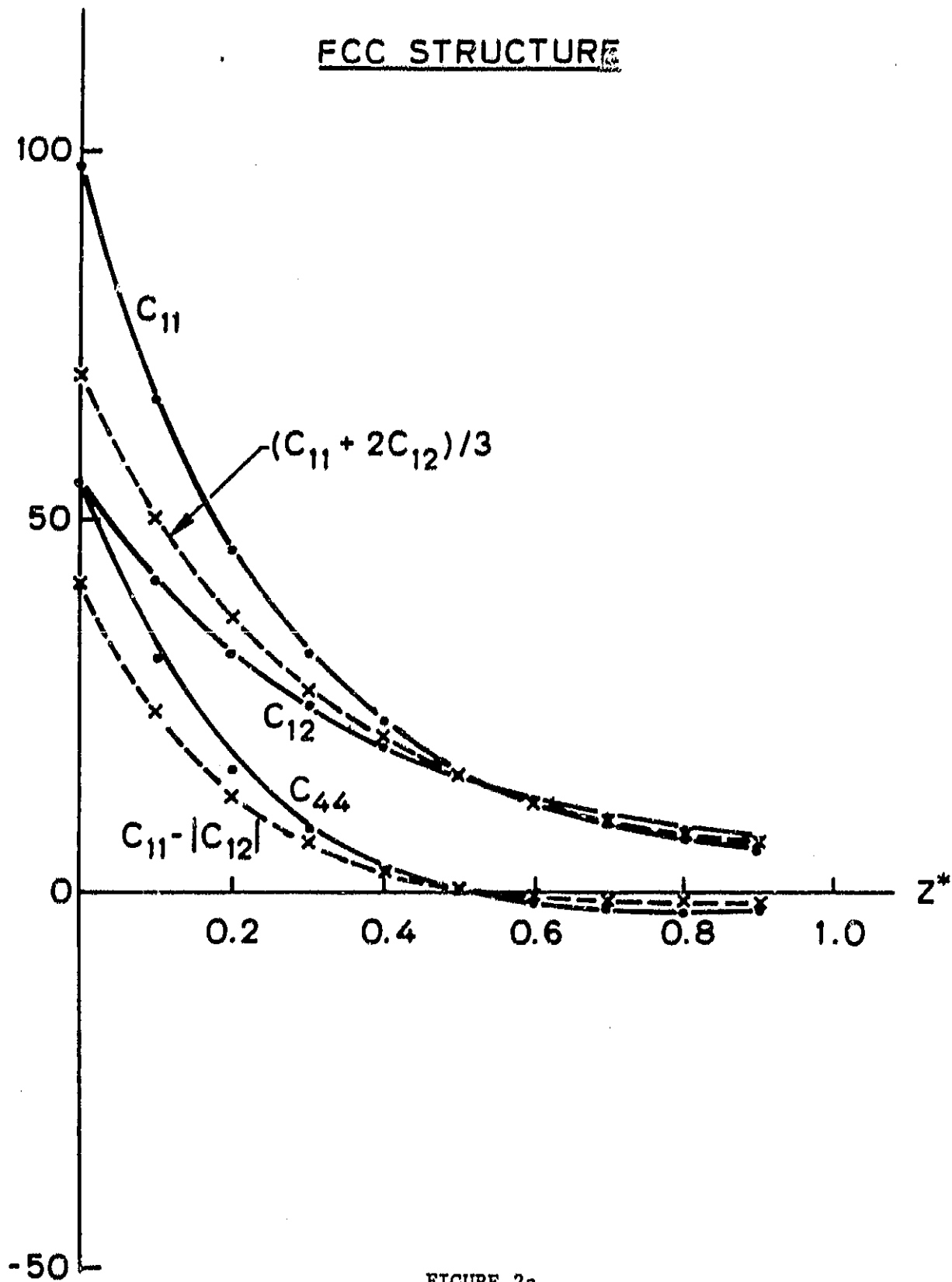
o

r

θ_j

r_{ij}

o

1

θ_l

x^2

θ_i

r_{1i}

$i\,(x_i^1\,x_i^2\,x_i^3)$
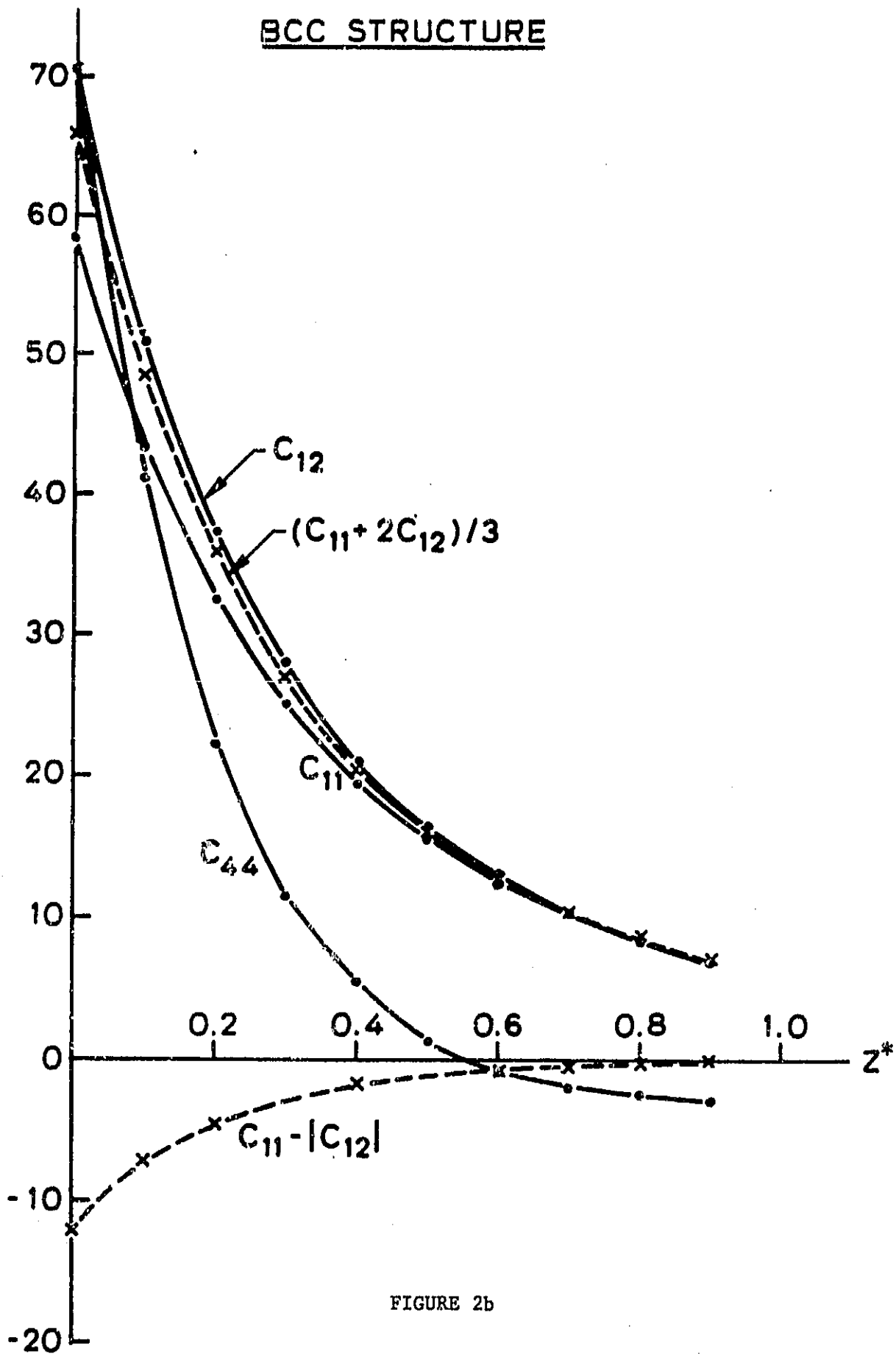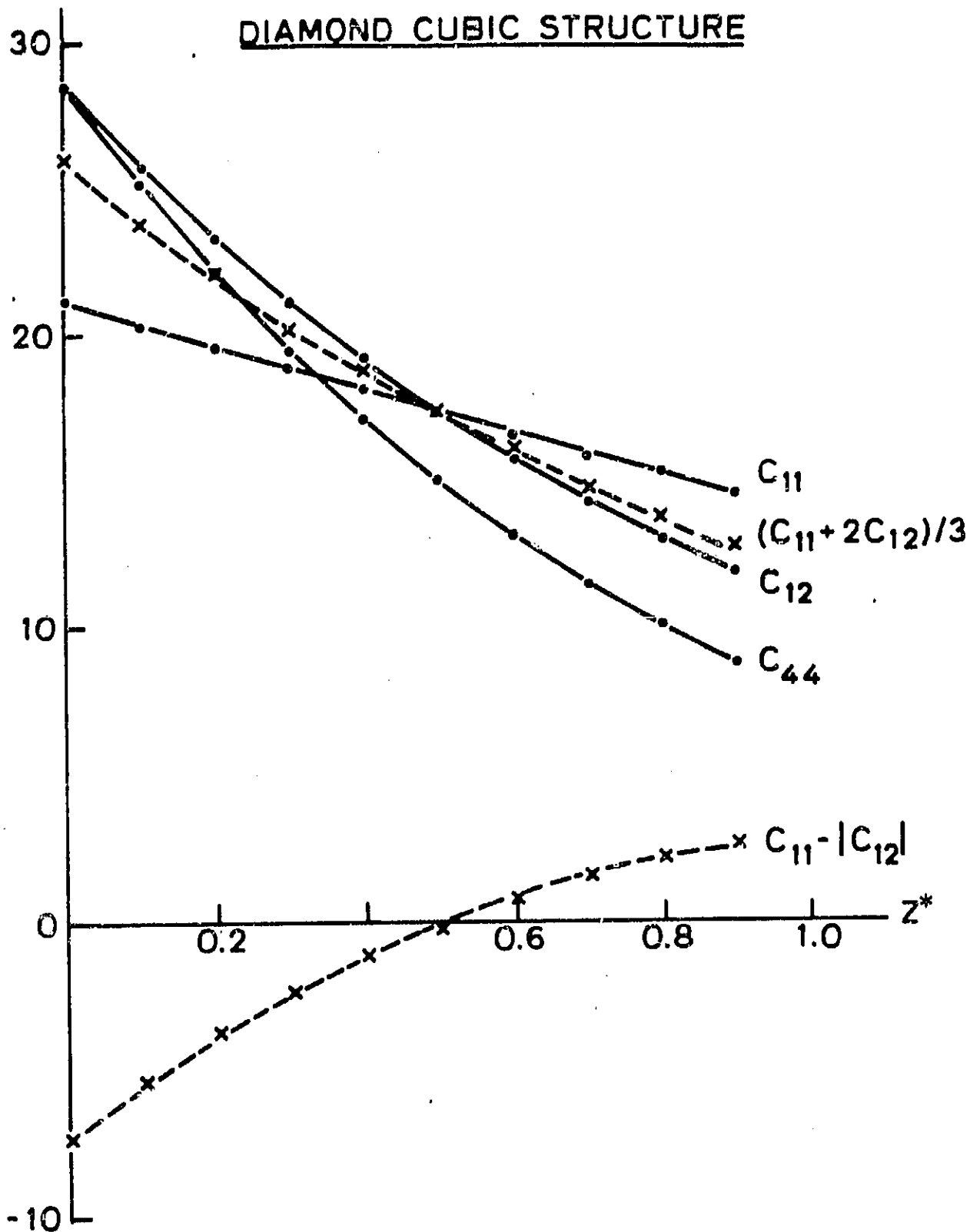
x^1

O

FIGURE 1

FCC STRUCTURE

FIGURE 2a

40
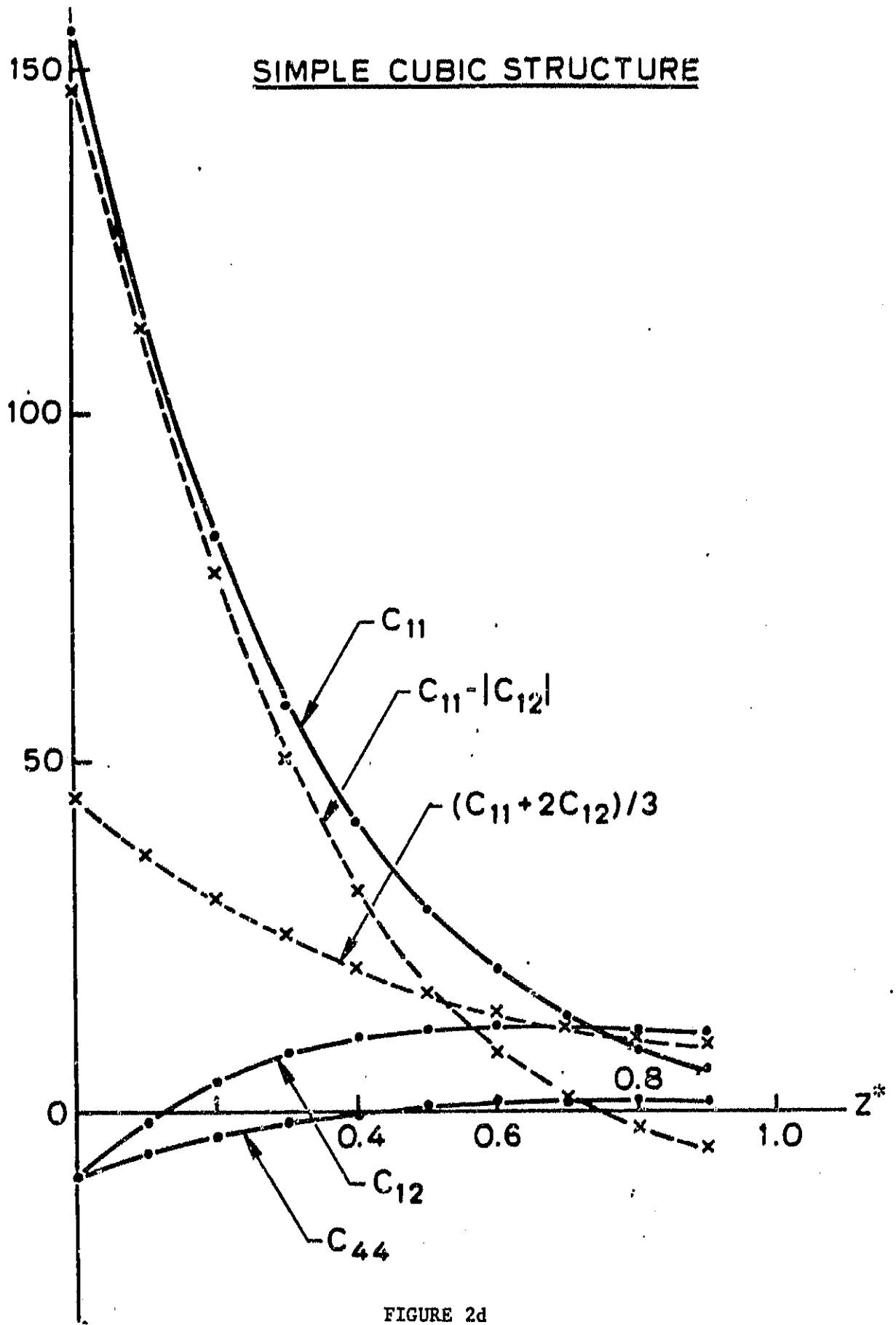
BCC STRUCTURE

FIGURE 2b

FIGURE 2c

SIMPLE CUBIC STRUCTURE
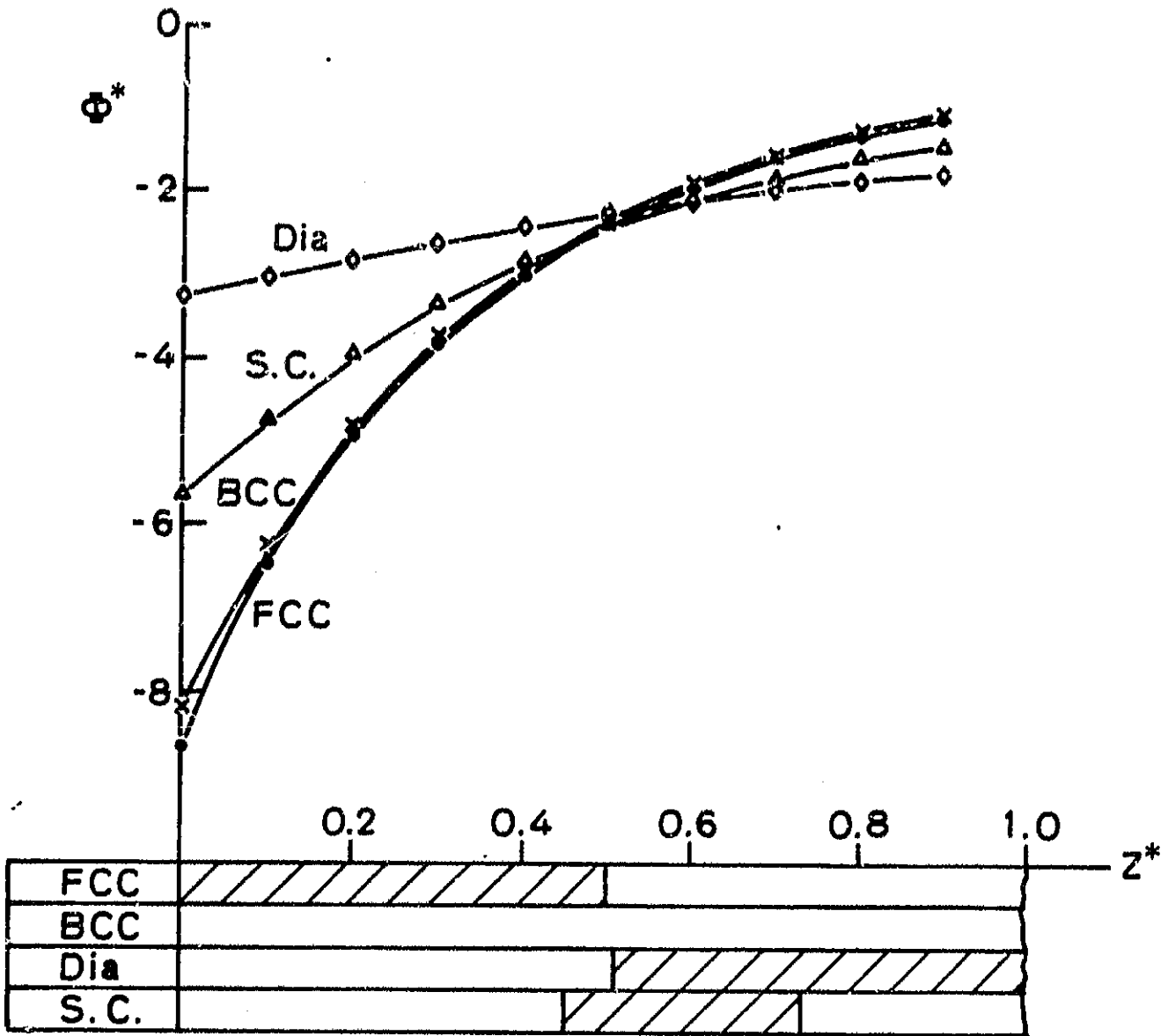
FIGURE 2d

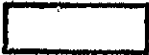43

FIGURE 3

44

Chapter III

CALCULATION OF POTENTIAL ENERGY PARAMETRES
FOR THE SILICON - CARBON SYSTEMS

Introduction

In simulation calculations, the functional simplicity as well as the reliability of a potential energy expression are both important considerations. In general, in such modeling investigations based on simple two-body interactions, the close-packed structures (hcp or fcc) are the only energetically stable configurations. Less dense structures (such as diamond cubic), on the other hand, are not stable with a potential energy function expressed as the sum of pair interactions only. This fact has been demonstrated in a recent parametric study on the stability of the diamond cubic crystal [1]. It has been determined that multi-body interactions are absolutely necessary; therefore, a potential energy function comprising two- and three-body terms (at least) must be employed for an adequate description of the diamond cubic structure.

In the present study, specific parameters of the potential energy functions for a variety of Si_p, C_q and Si_xC_y species are calculated and the applicability of the potential function, for reproducing various energetic and structural quantities was tested.

Analytical Procedure

A. Elemental Systems

For a system of N particles, in general, the total potential energy may be expanded as [2]:

$$\Phi = \phi_2 + \phi_3 + \cdots \tag{1a}$$

$$\phi_2 = \frac{1}{2!} \sum_{i}^{N} \sum_{\substack{j \\ i \neq j}}^{N} u(\vec{r}_i, \vec{r}_j) \tag{1b}$$

$$\phi_3 = \frac{1}{3!} \sum_{i}^{N} \sum_{\substack{j \\ i \neq j \neq k}}^{N} \sum_{k}^{N} u(\vec{r}_i, \vec{r}_j, \vec{r}_k) \tag{1c}$$

where, $u(\vec{r}_i, \vec{r}_j)$ and $u(\vec{r}_i, \vec{r}_j, \vec{r}_k)$ represent the two- and three-body interactions, respectively. The position of the i'th particle is denoted by $\vec{r}_i$.

In this study, the two-body part is represented by a Mie-type potential:

46

$$u(r_{ij}) = \frac{\epsilon}{(m-n)}\left[n(\frac{r_o}{r_{ij}})^m - m(\frac{r_o}{r_{ij}})^n\right] \tag{2}$$

where, $r_{ij} = |\vec{r}_i - \vec{r}_j|$; r_o represents the equilibrium distance and ϵ denotes the two-body energy at $r_{ij} = r_o$. The exponents m and n account for the repulsive and attractive terms, respectively. For the three-body term, the Axilrod-Teller equation is taken into consideration:

$$u(\vec{r}_i, \vec{r}_j, \vec{r}_k) = \frac{Z(1 + 3\cos\theta_i\cos\theta_j\cos\theta_k)}{(r_{ij} \cdot r_{ik} \cdot r_{jk})^3} \tag{3}$$

where, $\theta_i, \theta_j, \theta_k$ and r_{ij}, r_{ik}, r_{jk} represent the angles and the sides of the triangle formed by the three particles i, j and k, respectively. The three-body intensity parameter is denoted by Z. Interactions coming from higher body terms are neglected in this calculation. Considering the lattice sum formalism, next, the total potential energy function for a crystal is obtained by combining equations 1 through 3:

$$\Phi = \frac{N\epsilon}{2(m-n)}\left[nA(\frac{r_o}{d})^m - mB(\frac{r_o}{d})^n\right] + NZT_k(\frac{r_o}{d})^9 \tag{4a}$$

where, d represents the nearest neighbor distance and the lattice sums are given by:

$$A = \sum_j (\frac{d}{r_j})^m \tag{4b}$$

$$B = \sum_j (\frac{d}{r_j})^n \tag{4c}$$

and

$$T_k = \frac{1}{3!}\sum_j^N \sum_{\substack{k \\ j \neq k}}^N \frac{(1 + 3\cos\theta_i\cos\theta_j\cos\theta_k)d^9}{(r_{ij} \cdot r_{ik} \cdot r_{jk})^3} \tag{4d}$$

Numerical values for the lattice sums A, B and T_k for the diamond cubic crystal are given in reference [1].

B. Binary Species

For a binary system, equation 1a is replaced by

$$\Phi = \sum_{\alpha=1}^{2}\sum_{\beta=1}^{2}\phi_2(\alpha,\beta) + \sum_{\alpha=1}^{2}\sum_{\beta=1}^{2}\sum_{\gamma=1}^{2}\phi_3(\alpha,\beta,\gamma) \tag{5}$$

47

where, ϕ_2 and ϕ_3 are still given by eqs. 1b and 1c but now deal with the interactions between the species α and β and $\gamma (\gamma = \alpha$ or $\beta)$. For a binary crystal, we have

$$\phi_2(\alpha, \beta) = \frac{N_\alpha}{2(m_{\alpha\beta} - n_{\alpha\beta})} \epsilon_{\alpha\beta} \left[n_{\alpha\beta} A_{\alpha\beta} \left(\frac{r_{o(\alpha,\beta)}}{d} \right)^{m_{\alpha\beta}} - m_{\alpha\beta} B_{\alpha\beta} \left(\frac{r_{o(\alpha,\beta)}}{d} \right)^{n_{\alpha\beta}} \right] \quad (6a)$$

where

$$A_{\alpha\beta} = \sum_i^{N_\beta} \left(\frac{d}{r_{i(\alpha,\beta)}} \right)^{m_{\alpha\beta}} \quad (6b)$$

$$B_{\alpha\beta} = \sum_i^{N_\beta} \left(\frac{d}{r_{i(\alpha,\beta)}} \right)^{n_{\alpha\beta}} \quad (6c)$$

and

$$\phi_3(\alpha, \beta, \gamma) = \frac{N_\alpha Z_{\alpha\beta\gamma} T_{\alpha\beta\gamma}}{d^9} \quad (7a)$$

with

$$T_{\alpha\beta\gamma} = \frac{1}{3!} \sum_j^{N_\beta} \sum_{\substack{k \\ j \neq k}}^{N_\gamma} \frac{(1 + 3 \cos\theta_i^\alpha \cos\theta_j^\beta \cos\theta_k^\gamma) d^9}{(r_{ij(\alpha,\beta)} \cdot r_{ik(\alpha,\gamma)} \cdot r_{jk(\beta,\gamma)})^3} \quad (7b)$$

Subscripts i, j and k are the running indices, with similar definitions as the variables in eq. 4.

Pertinent lattice sums for several single component and binary systems are given in Tables 1 and 2 respectively. The following relationships hold for the two-component lattice sums

$$A_{11} = A_{22} \; ; \quad A_{12} = A_{21} \; ; \quad B_{11} = B_{22} \; ; \quad B_{12} = B_{21} \; ;$$

$$T_{111} = T_{222} \; , \quad T_{112} = T_{121} = T_{212} = T_{221} \; ; \quad T_{122} = T_{211} \quad (8).$$

C. Parameter Evaluation

In order for the potential energy function given by equations 1 through 3 to be used in a simulation calculation for a specific system, the parameters (ϵ, r_o and Z) must be first evaluated. In accordance with our earlier study, on the stability of the diamond cubic structure, the values of the exponents m and n were taken as 12 and 6, respectively. The evaluation process is basically a simple fitting procedure, however, due to the nonlinear nature of the potential function it often becomes quite cumbersome. Throughout this study only experimental data were employed in the evaluation of the parameters. Furthermore, one should remember that the

48

parameters, by definition, are independent of N and of the geometrical state of the system (i.e., independent of the particles' positions). They depend solely on the atomic species involved in the interaction.

In this study, parameters for pure Si and C as well as for the SiC system were evaluated. In each case, the basic experimental data for the crystalline bulk and for small clusters were taken into consideration. The data which are used in the calculation of the parameters are tabulated in Table 3. The evaluation procedure for the pure systems will be first outlined. The parameters for the homonuclear cases (Si and C) were calculated considering three basic restrictions. (i) The equilibrium criterion: at the static limit we have $\partial\Phi/\partial r_q = 0$; where, in the case of a crystal, r_q is the nearest neighbor distance and is directly related to the density. For small clusters, however, r_q represent internuclear distances between the particles. (ii) The stability region for the diamond cubic structure: according to results reported in reference [1] the parameter Z should satisfy: $0.55 < Z^* < 0.8$, where, Z^* is the reduced three-body intensity parameter defined as: $Z^* = Z/\epsilon r_o{}^9$. (iii)Stable trimer configuration: the energetically most favorable trimer configuration for a potential energy function defined by equations 1-3 has been investigated in reference [3]. Accordingly, if the trimer is linear, $0.68 < Z^*$ and, if it is (equilateral) triangular, $Z^* < 0.68$ must be satisfied.

The parameters for the homonuclear cases (Si and C) were selected in such a way that calculated energies for the small clusters (Si_3, C_3, Si_2 and C_2) and the crystalline states (silicon and diamond) exhibit a best fit to the corresponding experimental data. For this purpose the energies were calculated according to equations 1-3 using a series of parameter sets which obey the restrictions cited above. Numerical values of the best fitted parameters are given in Table 4.

In the case of the parameters for the SiC system, experimental data for SiC, Si_2C, SiC_2 molecules and for the crystalline β-SiC were used. The data consisted of the cohesive energy and the nearest neighbor distances for the bulk, and the bond energies along with the bond lengths for the small clusters. (See Table 3). Due to the binary nature of this system, in addition to the homonuclear interaction parameters, cross-parameters such as $\epsilon_{Si,C}$, $r_{o(Si,C)}$, $Z_{Si,Si,C}$ and $Z_{Si,C,C}$ needed to be determined.

In the evaluation of the cross-parameters for the β-SiC system, we also considered the following stability restrictions. (i) According to experimental data, Si_2C is a linear symmetrical molecule. Our present potential energy function satisfies this condition only if $Z^*_{(Si,Si,C)} > 0.41$ where,

$$Z^*_{(Si,Si,C)} = \frac{Z_{(Si,Si,C)}}{\left(\epsilon_{(Si,Si)}\epsilon_{(Si,C)}\epsilon_{(Si,C)}\right)^{1/3}\left(r_{o(Si,Si)}r_{o(Si,C)}r_{o(Si,C)}\right)^3} \tag{9}$$

(ii) On the other hand, experiments indicate that SiC_2 is also linear but asymmet-

49

rical and that it can only be stable if $Z^*_{(Si,C,C)} > 0.58$ with,

$$Z^*_{(Si,C,C)} = \frac{Z_{(Si,C,C)}}{\left(\epsilon_{(Si,C)}\epsilon_{(Si,C)}\epsilon_{(C,C)}\right)^{1/3}\left(r_{o(Si,C)}r_{o(Si,C)}r_{o(C,C)}\right)^3} \qquad (10)$$

(iii) For the crystalline β-SiC as well as for the SiC, Si_2C and SiC_2 molecules, the stability criterion which is given by $\partial\Phi/\partial r_q = 0$ should also be satisfied.

We employed the parameters for Si and C obtained above, and calculated energies for the crystalline β-SiC, and α-SiC, Si_2C and SiC_2 molecules for a series of cross-parameters sets. The best fitted cross-parameters with the above restrictions were chosen and tabulated in Table 4 along with the parameters for Si and C.

Discussion

In order to analyze how well the parameters can now reproduce experimental data, we plotted the experimental energies, versus the calculated values in figure 1. It is important to remember that, in this graph for each case, we used the same potential function associated with the same set of parameters given in table 4. The dotted line indicates the ideal positions (i.e., the 45° line). For such a large variety of systems (ranging from crystalline phases all the way down to isolated molecular species) the agreement obtained between the experimental and calculated energy values can be considered quite good. The plot also contains the energies for C_4, C_5 and crystalline graphite which were not included in the parameter evaluation procedure. While the energy value for graphite displays some ($\sim$ 30%) deviation, calculated energies for C_4 and C_5 are in very good agreement with the experimental values. Another important point related to figure 1 is the slight segregation of the energy values for different species. All the calculated energies for the bulk cystalline cases (namely, for silicon, diamond, graphite, α-silicon carbide(4H-III) and β-silicon carbide) were found to be somewhat lower than the corresponding experimental values, while all the small molecular species produced slightly higher energies. In general, the tendency for this sort of segregation in the case of a potential energy function based on two-body interactions only, is much more pronounced [4] than in the present case. This situation may be closely related to the effect of three-body interactions which are properly accounted for in our calculations via equation 3. The energies for α-SiC and β-SiC were found to be very close to each other (see Table 3), and they were considerably lower than the energies calculated for other structures (Table 2).

References

[1] See Chapter 1.

[2] T. Halicioğlu, phys. stat. sol. (b), **99**, 347 (1980).

[3] T. Halicioğlu and P. J. White, J. Vac. Sci. Technol., **17**, 1213 (1980).

[4] R. Dürer, Adv. Atomic and Molec. Physics, **16**, 55 (1980).

[5] I. Barin, O. Knacke, "Thermochemical Properties of Inorganic Substances", (Springer-Berlag, New York, 1973).

[6] R. Hultgren et al., "Selected Values of the Thermodynamic Properties of the Elements", (American Society for Metals, 1973).

[7] "JANAF Thermochemical Tables", 2nd edition, 1971 NSRDS-NBS 37, U. S. Department of Commerce, National Bureau of Standards.

[8] JANAF Table dated Mar. 31, 1961.

[9] R. W. G. Wyckoff, "Crystal Structures", 2nd edition, (John Wiley & Sons, New York, 1963) Vol. 1.

Figure Caption

Figure 1 Comparison of the calculated cohesive energies with the experimental values.

Table 1

Lattice Sums for the Mie and Axilrod-Teller Potentials for Various Structures.

	FCC	BCC	DIA	GRAPH	β-tin
B	14.4481	12.2495	5.1153	3.3895	8.2864
A	12.1319	9.1141	4.0089	3.0092	5.4654
T_k	19.1697	14.7719	1.6647	0.1010	7.0706

Table 2

Lattice Sums for two-component systems.

	NaCl structure	CsCl structure	ZnS structure	BN structure	α-SiC (4H-III)
A_{11}	0.1896	1.1038	0.0337	0.0084	0.0342
A_{12}	6.0126	8.0103	4.0045	3.0009	4.0595
B_{11}	1.8003	3.5357	0.7596	0.2821	0.7657
B_{12}	6.5888	8.6996	4.3516	3.1163	4.3893
T_{111}	2.5272	5.4138	0.6928	0.1057	0.7013
T_{112}	11.5117	25.8716	2.8595	0.1574	2.8967
T_{122}	5.7544	12.9374	1.4298	0.0787	1.4558

Table 3

Experimental and calculated energies and bond distances.

Species	Bond distances or nearest neighbor distance (Å)		Cohesive energy (eV/molecule)	
	Experiment	Calculation	Experiment[5,6,7,8]	Calculation
$Si_{2(g)}$	$2.246^{(7)}$	2.295	-3.208 ± 0.216	-2.817
$Si_{3(g)}$ linear	$2.25^{(7)}$	2.267	-7.407 ± 0.563	-6.247
$Si_{(s)}$ diamond cubic	$2.3516^{(9)}$	2.3516	-4.662 ± 0.043	-5.568
$C_{2(g)}$	$1.242^{(7)}$	1.4806	$-6.215^{+0.192}_{-0.130}$	-5.437
$C_{3(g)}$ linear	$1.277^{(7)}$	1.458	$-14.033^{+0.692}_{-0.067}$	-12.362
$C_{4(g)}$ linear	$1.28^{(7)}$	$r_1 = 1.44$ $r_2 = 1.455$	$-19.686^{+0.042}_{-0.434}$	-19.507
$C_{5(g)}$ linear	$1.28^{(7)}$	$r_1 = 1.435$ $r_2 = 1.455$	$-27.014^{+0.629}_{-0.369}$	-26.70
$C_{(s)}$ diamond cubic	$1.5445^{(9)}$	1.5445	$-7.394^{+0.074}_{-0.022}$	-9.402
$C_{(s)}$ graphite	$1.4180^{(9)}$	1.4619	$-7.415^{+0.074}_{-0.022}$	-9.807
$SiC_{(g)}$	$1.70^{(7)}$	1.74	$-4.631^{+0.464}_{-0.412}$	-3.894
$Si_2C_{(g)}$ symmetric linear	$1.75^{(7)}$	1.70	$-11.198^{+0.420}_{-0.378}$	-9.594
$C_2Si_{(g)}$ unsymmetric linear	C–C=$1.28^{(7)}$ C–Si=1.75	C–C=1.463 C–Si=1.711	$-13.128^{+0.494}_{-0.390}$	-10.510
β-$SiC_{(s)}$ zinc-blende	$1.8878^{(9)}$	1.8115	$-12.835^{+0.182}_{-0.130}$	-15.714
α-$SiC_{(s)}$ 4H-III	$1.885^{(9)}$	1.8135	$-12.817^{+0.182}_{-0.130}$	-15.736

Table 4
Potential Energy Parameters.

Two-body Parameters	(Si-Si)	(C-C)	(Si-C)
ϵ (eV)	2.817	5.437	3.895
r_0 (Å)	2.2951	1.4806	1.74

Three-body intensity parameter	(Si-Si-Si)	(C-C-C)	(Si-Si-C)	(Si-C-C)
Z (eV·Å^9)	3484.0	167.3	698.2	261.8